Nonequilibrium 2D-IR Exchange Spectroscopy: Ligand Migration in Proteins

J. Bredenbeck[1], J. Helbing[1], K. Nienhaus [2], G. U. Nienhaus [2,3] and P. Hamm[1]

[1] University of Zurich, Wintherthurerstrasse 190, 8057 Zurich, Switzerland
E-mail: j.bredenbeck@pci.unizh.ch
[2] University of Ulm, Albert-Einstein-Allee 11, 89081 Ulm, Germany
[3] University of Illinois at Urbana-Champaign, 1110 West Green Street, Urbana, IL 61801, USA

Abstract. 2D exchange spectroscopy maps networks of interconverting chemical species in dynamic equilibrium. We present the extension of ultrafast 2D-IR exchange spectroscopy to the nonequilibrium regime and its application to ligand migration in proteins.

1. Introduction

2D exchange spectroscopy (2D-EXSY) has been introduced in the field of nuclear magnetic resonance (NMR) already three decades ago [1]. Since then 2D-NMR-EXSY has grown into a powerful tool for mapping networks of chemical species that interconvert in equilibrium on a millisecond timescale. Recently, the concept of 2D-EXSY has been transferred to ultrafast vibrational spectroscopy, using 2D-IR pump probe [2] as well as 2D-IR echo techniques [3]. The sub-picosecond time resolution of 2D-IR-EXSY opens up a new range of exchange phenomena for real-time studies. While in a equilibrium 2D-IR-EXSY experiment exchange between species occurs spontaneously during the waiting time that separates the IR pulses, we present here an extension of 2D-IR-EXSY to triggered nonequilibrium systems.

2. 2D-IR exchange spectroscopy in and out of equilibrium

In pump-probe 2D-IR, a narrow-band IR_{pump} pulse is scanned across the absorption range of interest, defining the pump frequency axis of the 2D spectrum. After a waiting time τ, a broad-band IR_{probe} pulse measures the response of the sample, defining the probe frequency axis. Each vibration leads to a signal on the diagonal. If two chemical species x and y interconvert in dynamic equilibrium, and thereby change the frequency of a vibration during the waiting time τ, additional off-diagonal peaks are created by this exchange process. In this way, 2D-IR-EXSY maps connectivities by creating cross peaks between species connected by exchange. However, the 2D-EXSY concept is not limited to dynamic equilibrium, where exchange occurs spontaneously during the waiting time τ. Instead we can also trigger the exchange process by an additional UV/Vis_{pump} pulse applied during τ. In this fashion we can map interconversion of

species in a phototriggered nonequilibrium process, extending 2D-IR-EXSY to transient T2D-IR-EXSY.

3. Application to ligand migration in proteins

An exciting application where T2D-IR-EXSY can unfold its potential is the light triggered migration of ligands between different sites in a protein, such as the migration of the CO ligand in sperm whale myoglobin (sw-Mb). Mb is responsible for gas transport in muscle tissue. Besides CO it binds other small ligands like O_2 or NO. Associated with its function, the Mb:ligand complex features several conformational substates that coexist in solution. Different conformations show different bands in the ligand IR spectrum. CO at the *binding site* of sw-Mb displays two major bands that have been assigned to two conformations termed A_1 and A_3 [5, 6]. Upon photodetachment from the binding site, CO migrates to the primary *docking site* B, which mediates ligand transport to and from the binding site. Docked in B, the CO ligand again gives rise to several bands, B_2, B_1 and B_0 [5, 7, 8]. The issue we address here is the connectivity between A and B states, i. e. which A state dissociates into which B state. In the literature, B_2 and B_1 are attributed to reverse orientations of CO in the docking site of Mb in the A_1 conformation. B_0 has been assigned to the A_3 conformation [5]. An accompanying band due to a reverse CO orientation as for B_2 and B_1 has not yet been found for B_0. However, connections between A_3 and B_1/B_2 have been indicated [9].

To study the connectivities of A and B states by T2D-IR-EXSY, we selected the sw-Mb mutant V68Y featuring comparable populations of A_3 and A_1 [5]. As shown in Fig. 3a, 540 nm excitation detaches CO of both A substates from the heme iron. CO then enters the primary docking site B, populating B_2 , B_1 and B_0 (Fig. 3b). From this 1D data no conclusions can be drawn about the connectivity between A_3/A_1 and B_2/B_1/B_0. The connectivity information can, however, be obtained from appropriate cuts through the cross-peaks of the T2D-IR-EXSY spectrum as shown in Fig. 3d. For the upper, the IR_{pump} frequency has been set to the A_1 band, for the lower cut it has been set to A_3 (see arrows in Fig. 3c). The IR_{pump} pulse tags the CO by vibrational excitation before it starts migration to the B sites. Thus we find in the cross peak cuts depletion at the ω_{01} frequencies and an increased absorption at ω_{12}. The cuts for A_3 and A_1 look quite similar which would not be the case if A_3 converted exclusively to B_0 and A_1 to B_2 and B_1. Instead, the similar shape of the cuts at $\omega_{12}(B_2)$ and $\omega_{01}(B_2)$ shows that not only A_1 but also A_3 is connected to B_2. The horizontal brackets in the B-state spectrum Fig. 3e indicate the expected positions of the ω_{12} bands. In Fig. 3f, the cuts are overlaid to highlight their differences. The negative signal around the ω_{01} frequencies of B_1 and B_0 is blue shifted in the A_3 cut relative to the A_1 cut. This indicates that more B_0 is generated starting from the A_3 conformation. The positive ω_{12} contributions of B_1 and B_0 partially cancel the negative ω_{01} contribution of B_2 in both cuts. Also here, differences between the A_3 cut and the A_1 cut emerge. The amplitude of the A_3 cut is smaller around $\omega_{01}(B_2)$. This is another indication of the population of B_0 from A_3: $\omega_{12}(B_0)$ is closer to the ω_{01}

band of B_2 than the ω_{12} contribution of B_1, which leads to stronger cancellation in the A_3 cut. The solid lines in Fig. 3f accompanying the A_1 and A_3 cuts are simulations assuming the connectivities $A_1 \rightarrow (B_1,B_2)$, $A_3 \rightarrow (B_0,B_2)$ and take into account the finite width of the IR_{pump} pulse as well as the band overlap which limits the IR_{pump} selectivity on A_1 and A_3. These connectivities are well supported

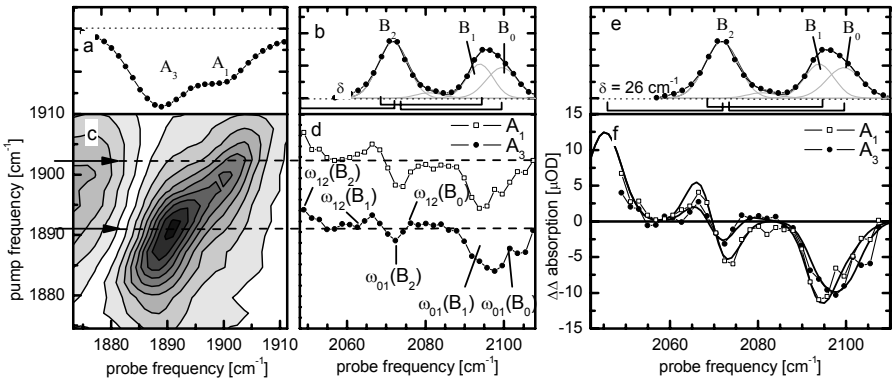

by the data.

Fig. 1. (a) TRIR spectrum of sw-Mb^{13}CO-V68Y, 5 ps after 540 nm excitation. (b) TRIR spectrum of CO in the B states, 5 ps after 540 nm excitation. (c) Conventional 2D-IR spectrum of the A_3 and A_1 state. (d) Cuts through the T2D-IR-EXSY cross peaks. IR_{pump} energies correspond to the arrows in (c). (e) Same as (c), rectangular brackets indicate the ω_{12} frequencies of the B_2, B_1 and B_0 bands. (f) Overlay of the cuts in (d). Solid lines accompanying the cuts: signal expected for the connectivities $A_1 \rightarrow (B_1,B_2)$, $A_3 \rightarrow (B_0,B_2)$.

In summary, T2D-IR-EXSY allowed us to track the migration of the CO ligand from the A to the B states in Mb and to establish their connectivity. We found that B_2 and B_1 are populated when starting from the A_1 substate. A_3 is also found to be connected not only to B_0 but also to B_2. A possible explanation is that B_2 actually consists of two bands, one being due to CO in the opposite orientation of B_1 as already known, and one being the elusive counterpart of B_0 featuring opposite CO orientation. This interpretation is supported by the finding of a splitting of B_2 in low temperature spectra [5].

References

1 B. H. Meier, R. R. Ernst, *J. Am. Chem. Soc.* 101, 6441, 1979

2 S. Woutersen, Y. Mu, G. Stock, P. Hamm, *Chem. Phys.* 266, 137, 2001

3 J. Zheng, K. Kwak, J. Asbury, X. Chen, I. R. Piletic, M. D. Fayer, *Science* 309, 1338, 2005

4 H. Frauenfelder, B. H. McMahon, P. W. Fenimore, *Proc. Natl. Acad. Sci.* 100, 8615, 2003

5 K. Nienhaus, P. Deng, J. S. Olson, J. J. Warren, G. U. Nienhaus, *J. Biol. Chem.* 278, 42532, 2003

6 J. Vojtechovsky, K. Chu, J. Berendzen, R. M. Sweet, I. Schlichting, *Biophys. J.* 77, 2153, 1999
7 K. Nienhaus, J. S. Olson, S. Franzen, G. U. Nienhaus, *J. Am. Chem. Soc.* 127, 40, 2005
8 M. Lim, T. A. Jackson, P.A. Anfinrud, *Science* 269, 962, 1995
9 J. R. Mourant, D. P. Braunstein, K. Chu, H. Frauenfelder, G. U. Nienhaus, P. Ormos, R. D. Young, *Biophys. J.* 65, 1496, 1993